Chem Soc Rev

Activation Strain Model and Molecular Orbital Theory: Understanding and Designing Chemical Reactions

Journal:	*Chemical Society Reviews*
Manuscript ID:	CS-REV-01-2014-000055.R1
Article Type:	Tutorial Review
Date Submitted by the Author:	20-Mar-2014
Complete List of Authors:	Fernandez, Israel; Universidad Complutense de Madrid, Organic Chemistry I Bickelhaupt, Matthias; VU University Amsterdam,

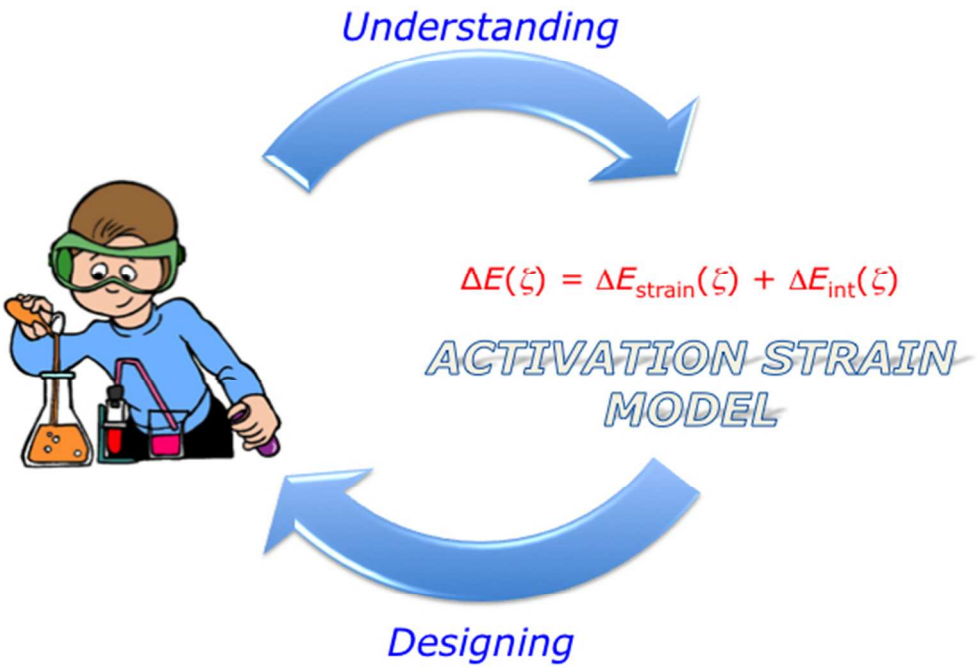

222x165mm (72 x 72 DPI)

Activation Strain Model and Molecular Orbital Theory: Understanding and Designing Chemical Reactions

Israel Fernández*[a] and F. Matthias Bickelhaupt*[b]

[a]Departamento de Química Orgánica I, Facultad de Ciencias Químicas, Universidad Complutense de Madrid, 28040, Madrid, Spain. E-mail: israel@quim.ucm.es
[b]Department of Theoretical Chemistry and Amsterdam Center for Multiscale Modeling (ACMM), VU University Amsterdam, De Boelelaan 1083, 1081 HV Amsterdam, and Institute for Molecules and Materials (IMM), Radboud University Nijmegen, The Netherlands. E-mail: f.m.bickelhaupt@vu.nl

Abstract

In this Tutorial Review, we make the point that a true *understanding* of trends in reactivity (as opposed to measuring or simply computing them) requires a causal reactivity model. To this end, we present and discuss the Activation Strain Model (ASM). The ASM establishes the desired causal relationship between reaction barriers, on one hand, and the properties of reactants and characteristics of reaction mechanisms, on the other hand. In the ASM, the potential energy surface $\Delta E(\zeta)$ along the reaction coordinate ζ is decomposed into the strain $\Delta E_{\text{strain}}(\zeta)$ of the reactants that become increasingly deformed as the reaction proceeds, plus the interaction $\Delta E_{\text{int}}(\zeta)$ between these deformed reactants, i.e., $\Delta E(\zeta) = \Delta E_{\text{strain}}(\zeta) + \Delta E_{\text{int}}(\zeta)$. The ASM can be used in conjunction with any quantum chemical program. An analysis of the method and its application to problems in organic and organometallic chemistry illustrate the power of the ASM as a unifying concept and a tool for rational design of reactants and catalysts.

Key learning points:

(1) *Understanding* trends in reactivity requires a causal reactivity model.
(2) The Activation Strain Model (ASM) establishes a causal relationship between reaction barriers, on one hand, and the properties of reactants and characteristics of reaction mechanisms, on the other hand.
(3) Reactivity trends depend on the capability of reactants to interact, on the distortivity (extent of deformation) associated with a reaction mechanism, and on the reactants flexibility, i.e., the ability to undergo this characteristic distortion.
(4) Activation Strain Analyses yield design principles for chemical reactions.

1. Introduction.

As defined by Linus Pauling, *"Chemistry is the science of substances: their structure, their properties, and the reactions that change them into other substances"*.[1] The latter aspect, molecular reactivity, is especially significant not only for the necessary advance of scientific knowledge but also because molecules play an important role in our everyday lives. Indeed, molecules derived from synthesis have even changed our way of living in many instances, as nicely illustrated by Nicolaou and Montagnon under the suggestive title of "Molecules that Changed the World".[2]

Therefore, a core task of Chemistry is the design and utilization of new molecules and synthetic routes towards these molecules. We all know that the rational design of efficient transformations (i.e., leading to the target molecule in quantitative or very high reaction yields without forming side products) necessarily implies an *a priori* detailed understanding of the physical factors which govern the relative heights of reaction barriers of the competing pathways. However, in most cases, synthetic (and also theoretical) chemists optimize the reaction conditions *a posteriori* based on trial & error procedures mainly because those factors controlling the intrinsic reactivity of molecules are incompletely understood prior to conducting the reaction of interest.

Here is the point where Theory is particularly helpful. Indeed, understanding what is behind a chemical reaction has been the goal of many theories and concepts. For instance, Woodward-Hoffmann rules,[3] Fukui's frontier molecular orbital (FMO) theory,[4] Valence-Bond analyses,[5] or Marcus theory[6] have enormously contributed to the current understanding of fundamental processes in chemistry and many of their principles and concepts have nowadays entered into the toolkit of many synthetic chemists.

In this Tutorial Review, we present a different computational approach to design, known as activation strain model (ASM), which can be used in conjunction with any quantum

chemical program. The ASM aims at a deeper understanding, both quantitative and qualitative, of the physical factors that control how the activation barriers arise in different fundamental processes. It does so by establishing a causal relationship between the height of reaction barriers, on one hand, and properties of the reactants and characteristics of the reaction mechanism, on the other hand (see Section 2). To this end, besides the description of the method and practical recommendations on its usage, we provide representative applications to reactions within organic and organometallic chemistry to illustrate that the insight gained with this approach complements and even modifies our current view of many fundamental processes. In addition, in some cases this insight has allowed us to design more efficient processes, which constitutes the ultimate task of chemists working on reactivity.

2. Activation Strain Model

The *activation strain model* (ASM),[7] also known as *distortion/interaction model*,[8] has allowed us to gain more insight into the physical factors which control how the activation barriers arise in different fundamental processes.[9] The method is a fragment approach to understanding chemical reactions, in which the height of reaction barriers is described in terms of the original reactants. The ASM is a systematic further development of the fragment approach, which was already used for stable molecules in a quantitative analysis scheme by Morokuma,[10] from equilibrium structures to transition states (TS) as well as *non-stationary* points, e.g., points along a reaction coordinate. Thus, in this model, the potential energy surface $\Delta E(\zeta)$ can be decomposed into two contributions along the reaction coordinate ζ: the strain (or distortion) energy $\Delta E_{\text{strain}}(\zeta)$, which is associated with the structural deformation that the reactants undergo, plus the interaction $\Delta E_{\text{int}}(\zeta)$ between these increasingly deformed reactants:

$$\Delta E(\zeta) = \Delta E_{strain}(\zeta) + \Delta E_{int}(\zeta) \quad (1)$$

The strain $\Delta E_{strain}(\zeta)$ is determined by the rigidity of the reactants and the extent to which groups must reorganize in a particular reaction mechanism. Therefore, this geometrical deformation is characteristic for the reaction pathway under consideration. In general, $\Delta E_{strain}(\zeta)$ is positive, that is, destabilizing, and thus a factor that gives rise to the occurrence of a reaction barrier. This term can be further partitioned into the individual contributions stemming from each of the reactants involved in the process.

The interaction $\Delta E_{int}(\zeta)$ between the reactants depends on their electronic structure and on how they are mutually oriented as they approach each other. Thus, the latter term is related to the bonding capabilities and mutual interaction between the increasingly deformed reactants along the same pathway. In most cases, $\Delta E_{int}(\zeta)$ is negative, that is, stabilizing, and therefore a factor that counteracts the strain term $\Delta E_{strain}(\zeta)$ and causes the eventual height of the reaction barrier to become lower than if strain would be the only actor. At this point, we wish to stress, however, that there are many exceptions to this rule. One example is provided by cycloadditions which feature positive, repulsive interaction terms in early stages of the reaction (see Section 3.2).

It is the interplay between $\Delta E_{strain}(\zeta)$ and $\Delta E_{int}(\zeta)$ that determines if and at which point along ζ a barrier arises. For instance, in the TS the reaction profile reaches its maximum, therefore satisfying $d\Delta E_{strain}(\zeta)/d\zeta = -d\Delta E_{int}(\zeta)/d\zeta$. The reaction coordinate, $\zeta$is usually obtained as the intrinsic reaction coordinate (IRC)[11] from a steepest-descent calculation. This reaction coordinate may then be projected onto a critical geometrical parameter, such as, the C···C bond that is formed during a Diels-Alder cycloaddition reaction as shown in Figure 1. The critical geometry parameter ζ is always defined at the x-axis of the diagram showing

$\Delta E(\zeta)$, $\Delta E_{strain}(\zeta)$ and $\Delta E_{int}(\zeta)$ as a function of the progress of the reaction, ζ, the so-called activation strain diagram (ASD).

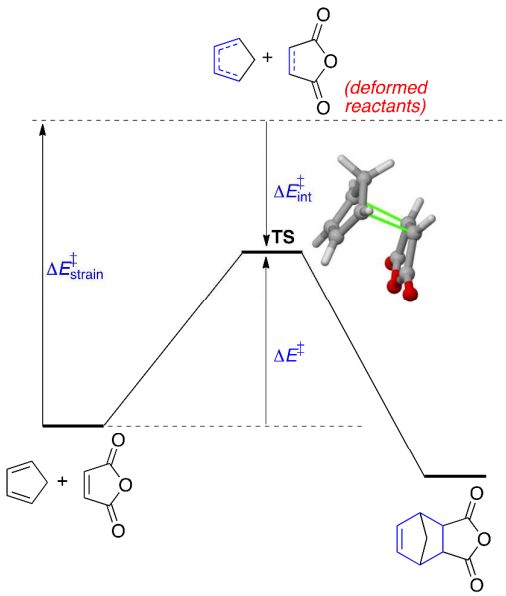

Figure 1. Illustration of the activation strain model ($\Delta E^{\ddagger} = \Delta E^{\ddagger}_{strain} + \Delta E^{\ddagger}_{int}$) using the endo-pathway of the Diels-Alder cycloaddition reaction between cyclopentadiene and maleic anhydride.

According to this model, the activation energy of a reaction $\Delta E^{\ddagger} = \Delta E(\zeta^{TS})$ consists of the activation strain $\Delta E^{\ddagger}_{strain} = \Delta E_{strain}(\zeta^{TS})$, which is defined as the energy we need to deform the reactants from their equilibrium geometries to the geometries they adopt in the corresponding TS, plus the TS interaction $\Delta E^{\ddagger}_{int} = \Delta E_{int}(\zeta^{TS})$ (see Figure 1). Therefore, $\Delta E^{\ddagger} = \Delta E^{\ddagger}_{strain} + \Delta E^{\ddagger}_{int}$.

The values of $\Delta E^{\ddagger}_{strain}$ and $\Delta E^{\ddagger}_{int}$ at the TS must be interpreted with great care, since the optimized TS structure is the result of a balance of the components $\Delta E_{strain}(\zeta)$ and $\Delta E_{int}(\zeta)$. This highlights the importance of taking into account the behaviour of the two components along the reaction coordinate, especially their slopes. *A single-point analysis at the TS, only, yields values that can be misleading!*

To illustrate this, please consider the activation strain diagrams for two generic reactions A and B (Figure 2). It is clear that reaction B proceeds with a lower activation

barrier. A single-point analysis at the respective transition states may suggest that this is due to a lower activation strain for reaction B, not because of a more stabilizing TS interaction. After all, the TS interaction is actually slightly less stabilizing, that is, less negative at the TS for reaction B than at the TS for reaction A. This suggests that the mutual bonding capability of the reactants in reaction B is reduced but that the barrier is nevertheless lower because of a lower rigidity or a less distortive character of the reaction as compared to reaction A. However, if we consider the complete analysis and not only the TS region, we will realize that this conclusion is not correct! The interaction ΔE_{int} of reaction B is clearly *more stabilizing at any given point along the reaction coordinate* than ΔE_{int} of reaction A. The fact that this seems to be reversed in the single-point analyses is due to the fact that the TS structures of A and B occur at different locations along the reaction path. Therefore, an important lesson is to be learnt from this illustrative case: we should be really cautious when comparing the single-point energies of TS's occurring at different points along the reaction coordinate.

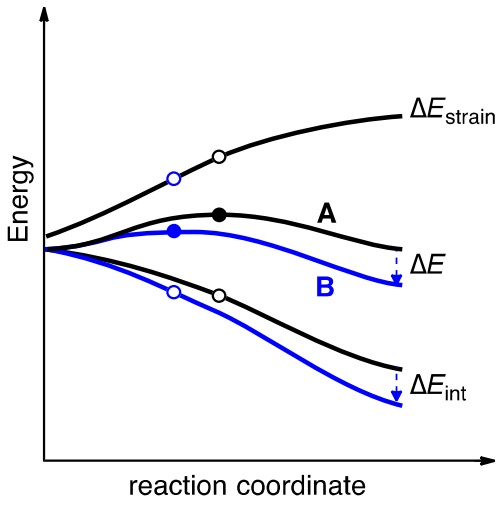

Figure 2. Schematic activation strain diagrams (ASD) for arbitrary reactions A (black curves) and B (blue curves) with identical strain ΔE_{strain} (black curve). From reaction A to B, the interaction energy becomes more stabilizing which lowers the TS (indicated by a dot) and shifts it towards the educt side, on the left.

The interaction ΔE_{int} between the deformed reactants can be further analysed in the conceptual framework provided by the Kohn-Sham molecular orbital model using the so-

called Energy Decomposition Analysis (EDA) method.[10] Within this method, initially developed by Ziegler and Rauk following a similar procedure suggested by Morokuma, the interaction energy $\Delta E_{int}(\zeta)$ is further decomposed into the following energy contributions:[10]

$$\Delta E_{int}(\zeta) = \Delta V_{elst}(\zeta) + \Delta E_{Pauli}(\zeta) + \Delta E_{oi}(\zeta) + \Delta E_{disp}(\zeta) \quad (2)$$

The term ΔV_{elst} corresponds to the quasiclassical electrostatic interaction between the unperturbed charge distributions of the deformed reactants and is usually attractive. The Pauli repulsion ΔE_{Pauli} comprises the destabilizing interactions between occupied orbitals and is responsible for any steric repulsion. The orbital interaction ΔE_{oi} accounts for charge transfer (interaction between occupied orbitals on one moiety with unoccupied orbitals of the other, including the HOMO–LUMO interactions) and polarization (empty–occupied orbital mixing on one fragment due to the presence of another fragment). This term can be further decomposed into contributions from different symmetries, such as, σ-, π- and δ-orbital interactions.[10a,b] Finally, ΔE_{disp} takes into account the interaction due to dispersion forces. Further details about the EDA method can be found in the literature.[10]

Before going into details, just a few final practical considerations:

(i) As stated above, the activation strain analyses are carried out along the reaction coordinate from the separate reactants (i.e. from infinity) to the reaction products via the corresponding transition state. Consequently, all energy curves should start, on the reactant side, at zero kcal/mol. However, if a reaction complex can be located on the potential energy surface, this species is recommended as the starting point for the activation-strain analysis. Hence, the energy curves will start at a point in the diagram where the reaction coordinate ζ is already slightly larger than zero and the reactants do already (weakly) interact and deform each other, i.e., $\Delta E(\zeta)$, $\Delta E_{strain}(\zeta)$, and $\Delta E_{int}(\zeta)$ may already slightly deviate from zero (see figures later on).

(ii) After obtaining the reaction profile (through an IRC calculation), any quantum mechanical program package is able to perform an activation strain analysis. This only requires two extra single-point computations per step along the reaction coordinate, namely, each of the two individual reactants in the geometry they adopt at that point. However, the quantitative energy decomposition scheme for ΔE_{int} described above, in particular, the decomposition of the orbital-interaction term into contributions from different symmetries (e.g., σ-, π- and δ-orbital interactions), has only been implemented in the Amsterdam Density Functional (ADF) program package.[12]

3. Representative Reactions

In this section, we shall describe representative reactions where the ASM has been particularly helpful to understand the physical factors controlling the activation barriers and trends in reactivity of fundamental processes in Chemistry. The considered processes in this section span from relatively simple textbook reactions like S_N2 or E2 reactions to transition metal mediated bond activation reactions.

3.1. S_N2 Reactions

3.1.1. S_N2 involving main group elements

As we all know, the term bimolecular nucleophilic substitution (S_N2) reactions, initially introduced by Ingold, Hughes and co-workers,[13] refers to processes which involve the synchronous displacement of an atom/group (the leaving group) by another atom/group (the nucleophile). This type of transformations is ubiquitous in Chemistry and plays a significant role in areas ranging from inorganic and organic till biological processes. The original

definitions of the terms S_N1, S_N2, E1 and E2 are accurate enough to characterize key aspects of the reaction mechanisms involved.[13] On the other hand, despite the great number of experimental and theoretical efforts carried out to gain insight into these fundamental processes, the precise factors responsible for trends in rates, mutual competition and other mechanistic details of these reaction types have been incompletely understood up till the last decades and even up till the present.

With this scenario, we decided to study the main factors which influence S_N2 reactions using the ASM. Thus, the nucleophilicity of X^-, leaving-group ability of Y, role of central atom, effect of substituents R as well as solvent effects were covered in detail (Scheme 1).[14,15,16]

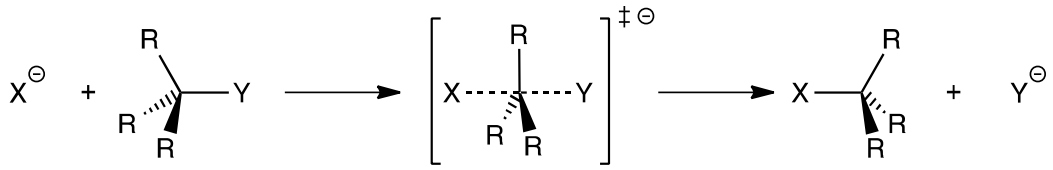

Scheme 1. S_N2 reaction.

Two possible mechanisms can be envisaged for this process: (a) via a backside attack with inversion of configuration (also known as Walden inversion), and (b) via a frontside attack, which would proceed with retention of configuration (Figure 3). In general, it was found that the backside S_N2 is favoured because of: (i) the sterically less favourable proximity of the larger and more electronegative nucleophile and leaving group in the frontside pathway; and (ii) the fact that the nucleophile lone-pair HOMO overlaps and interacts more favourably with the large backside lobe of the substrate's σ^*_{C-Y} LUMO than with this orbital's frontside region which features the nodal surface stemming from the antibonding combination between C and Y.[16] However, this overlap effect and the associated weakening in the interaction term are less important for the preference of backside over frontside S_N2

substitution than the steric crowding in the latter transition state mentioned above. This crowding translates into an increased strain which raises the barrier as shown in Figure 4 when changing from "reaction A" (which in this example stands for backside S_N2) to "reaction C" (corresponding here to frontside S_N2).

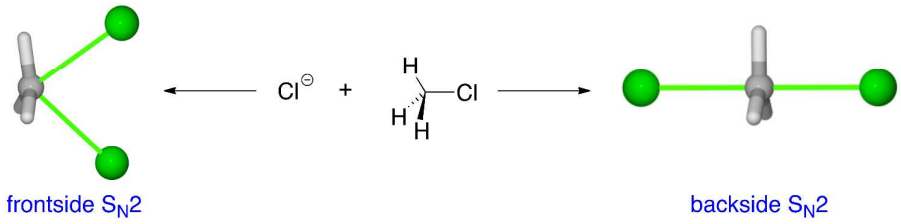

Figure 3. Backside and frontside S_N2 transition states for $Cl^- + CH_3Cl$.

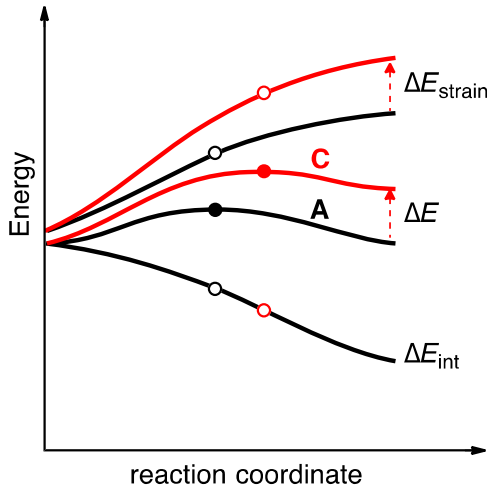

Figure 4. Schematic activation strain diagrams (ASD) for arbitrary reactions A (black curves) and C (red curves) with identical interaction ΔE_{int} (black curve). From reaction A to C, the strain energy becomes more destabilizing which raises the TS and shifts it towards the product side, on the right.

Thus, the ASM reveals that the central barrier of nucleophilic substitution at carbon (S_N2@C) is steric in nature:[14,15] it arises from the steric congestion that occurs in the S_N2 transition state in which five substituents try to approach the relatively small carbon atom. For the more favourable backside attack, the steric (Pauli) repulsion that occurs between these five substituents as the nucleophile X^- approaches causes deformations in the substrate CR_3Y:

the C–R bonds bend away from the approaching nucleophile and the C–Y bond elongates. Thus, the three C–R bonds flip over as the LG leaves, much like an "umbrella turning" in a strong wind. The geometrical deformation induced by steric interactions shows up in a relatively high strain energy. Note that the geometrical deformations in the S_N2 transition state relieve and therefore mask the steric repulsion which caused them in the first place. In other words, the steric (Pauli) repulsion that would otherwise occur in the interaction ΔE_{int} between the reactants, is transformed into strain energy ΔE_{strain} within the reactants.

This steric congestion in the S_N2 transition state decreases drastically if one goes from substitution at the small carbon atom, e.g., in $Cl^- + CH_3Cl$ (S_N2@C), to substitution at the larger silicon atom, e.g., in $Cl^- + SiH_3Cl$ (S_N2@Si), which allows for more space between the five substituents in the five-coordinate transition state.[14,15] Consequently, the strain curve drops. Together with a more favourable interaction between the reactants occurs in the S_N2@Si reaction, the net result is that the central barrier disappears, turning the five-coordinate transition species into a stable "transition complex" in the case of silicon as the central atom (Figure 4). Interestingly, the "carbon behaviour", which is characterized by substitution proceeding via a central barrier, reappears as the steric hindrance around the silicon atom increases (along the model reactions $Cl^- + Si(CH_3)_3Cl$ and $Si(OCH_3)_3Cl$) mainly because the strain curve, ΔE_{strain}, is significantly raised. Similar results have been observed when the substitution reaction occurs at phosphorous as central atom (S_N2@P): the central barrier disappears because there is less steric congestion and a more favourable interaction in the model reaction $Cl^- + PH_2Cl$, whereas it reappears again as the steric bulk around the phosphorus atom is raised (e.g. along $Cl^- + POH_2Cl$, $PO(CH_3)_2Cl$, and $PO(OCH_3)_2Cl$ reactions).[17]

In addition, electronic effects, such as the mutual bonding capabilities of the reactants as well as their internal bonding or rigidity, have a strong influence on the height of the S_N2

barrier. For instance, our activation strain analyses on the reaction between halides and halomethanes show that nucleophilicity directly and straightforwardly depends on the electron donating capability of the nucleophile:[16] a higher-energy n*p* atomic orbital on the halide X^- causes more stabilizing interactions ΔE_{int} with the substrate and thus a lower S_N2 barrier, as illustrated by Figure 2. On the other hand, a stronger carbon–leaving-group (C–Y) bond translates directly into a more destabilizing strain curve ΔE_{strain} and therefore into a higher S_N2 barrier, as illustrated by Figure 4.

The above findings suggest that the barrier of the S_N2 reactions can be efficiently controlled by modifying the interplay between the strain and interaction energies, which in turn, depends directly on the nature of the nucleophile, nucleofugue, central atom and its substituents. Indeed, the S_N2@C transition state can be "frozen" in hypervalent species of the type $[X–C(CN)_3–X]^-$ (X = Br, I, At) which, instead of being labile saddle-point structures, are predicted to be stable minima on the potential energy surface.[18]

The stabilization of the incipient negative charge in the five-coordinate species plays therefore a crucial role to transform the expected transition structure into a stable intermediate. This has been studied in detail in nucleophilic substitution reactions at carbon atoms involved in aromatic systems (S_NAr)[19] and double bonds (S_NV)[20] covering a good number of nucleophiles and nucleofugues along the periodic table. In these transformations, the electronic nature of the π-system controls the formation of stable "five-coordinated" carbon atom species, the so-called Meisenheimer intermediates. The factors governing the Meisenheimer/central-barrier dichotomy have been unravelled using the ASM and molecular orbital (MO) theory. In a nutshell, it was found[19,20] that the intrinsic nucleophilicity in S_NAr reactions is very different from the nucleophilicity in S_N2 processes.[14,16,21] Moreover, periodic trends for $S_NV\pi$ are essentially the same as for S_NAr, while intrinsic $S_NV\sigma$ nucleophilicity

parallels aliphatic S_N2. In conclusion, there appears to be no universal nucleophilicity scale valid for all types of nucleophilic substitution reactions.

It becomes therefore clear that an apparently simple textbook reaction like the bimolecular substitution reaction is subjected to a subtle balance between steric and electronic effects. As shown by the ASM, while the central barrier of S_N2 reactions has a steric origin, one could design low barrier reactions by attenuating the strain energy ΔE_{strain} and/or by strengthening the interaction energy ΔE_{int} between the deformed reactants.

3.1.2. S_N2 versus E2 Competition

In bimolecular 1,2-eliminations (E2) an anionic base abstracts a proton from the β-carbon center of a substrate molecule while, simultaneously, a leaving group (LG) at the α-position is released.[13] Therefore, S_N2 and E2 reactions share a number of similarities: both require good leaving groups, and both proceed concertedly. As good nucleophiles are often strong bases too, the two reactions often compete with each other.

In general, it is found that (i) E2 elimination is favoured by strong bases, (ii) acid catalysis which involves a comparatively weak, neutral base or nucleophile in general goes with substitution, whereas (iii) basic conditions, often featuring stronger, anionic bases, tune reactivity towards elimination. In order to gain insight into the electronic mechanism behind the observed shift from substitution to elimination if one goes from acidic to more basic conditions, we very recently decided to apply the ASM to the following model reactions:[22]

$$H_2O + CH_3{-}CH_2OH_2^+ \rightarrow H_3O^+ + CH_2{=}CH_2 + H_2O \quad (3)$$

$$H_2O + CH_3{-}CH_2OH_2^+ \rightarrow CH_3{-}CH_2OH_2^+ + H_2O \quad (4)$$

$$OH^- + CH_3{-}CH_2OH \rightarrow H_2O + CH_2{=}CH_2 + OH^- \quad (5)$$

$$OH^- + CH_3{-}CH_2OH \rightarrow CH_3{-}CH_2OH + OH^- \quad (6)$$

These reactions correspond to elimination and substitution under extremely acidic (Eqs. 3 and 4) and basic conditions (Eqs. 5 and 6), respectively. From the data in the corresponding activation strain diagrams (Figure 5), it becomes clear that the changes in strain and interaction if we go from acidic to basic conditions are significantly larger for the elimination pathway. Thus, while in the acidic case the strain and interaction curves do not differ much for elimination and substitution, they adopt significantly larger absolute values for elimination under basic conditions. Despite that, the single most determining factor working in the direction of the overall shift in preferential reactivity from nucleophilic (substitution) to protophilic reactivity (elimination) is an enormous gain in stabilizing interaction between the reactants if one goes to basic conditions, in particular in the case of elimination. An important reason behind this shift in interaction in favour of protophilic attack is the change in character of the substrates LUMO from C^{β}–H bonding to C^{β}–H antibonding which promotes β-proton transfer from substrate to electron-donating reactant, as explained in more detail in Ref. 22.

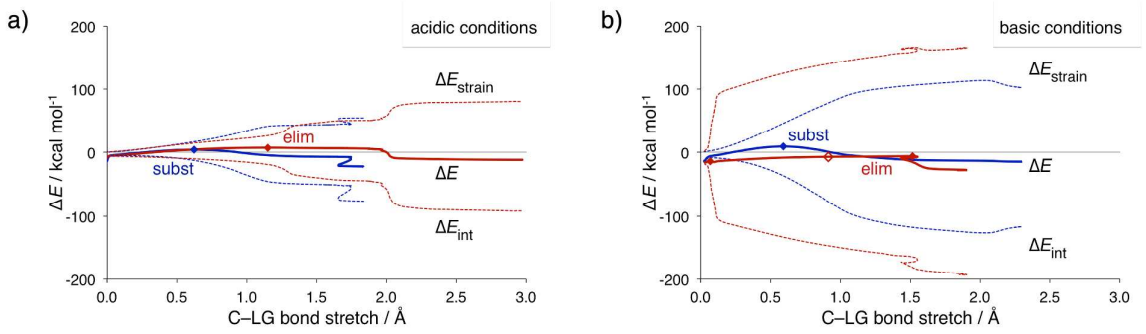

Figure 5. Activation strain analyses show that S_N2 *vs.* E2 competition (blue *vs.* red curves) shifts from substitution under acidic to elimination under basic conditions.

The competition between S_N2 and E2 pathways for a range of anionic bases reacting with ethyl chloride has been also studied by Wu and co-workers.[23] Similarly to our earlier findings,[7] it is confirmed that the E2 pathway, despite a more distortive character and higher activation strain $\Delta E^{\ddagger}_{strain}$, dominates the S_N2 pathway in the gas phase because of a more

stabilizing TS interaction $\Delta E^{\ddagger}_{int}$. In addition, Yun et al. rationalized the preference of hydride attacks on different positions on aziridinium ions via differences in activation strain in the transition states, related to the relative amount of stretch of the carbon–leaving-group bond in the transition states.[24]

3.1.3. S_N2 involving transition metals: Oxidative Addition

S_N2 reactions are important not only in organic chemistry but also in homogeneous catalysis. A point in case is C–X bond activation via oxidative addition to a transition-metal centre. This reaction would fit perfectly in Section 3.3 on transition-metal mediated bond activation but we choose to discuss it already here, in order to emphasize the structural and electronic resemblance between the corresponding transformations in organic and organometallic chemistry.

Oxidative addition is the rate-limiting step of a good number of cross-coupling reactions. This process involves cleaving the C–X bond and forming two new coordination bonds at the transition metal (TM), thus increasing its oxidation state by two units.[25] Two main mechanisms have been proposed for this fundamental reaction: (a) the concerted pathway, which involves the simultaneous formation of the TM–C and TM–X bonds in the transition state, and (b) an S_N2-type mechanism, where the central carbon atom is attacked by the transition metal expelling X^- and forming a cationic species; subsequently, both charged species combine to yield the product (Scheme 2).[25] The difference between both reaction pathways is important since, similarly to the back- and frontside nucleophilic attack (see above), it corresponds to a change in stereochemistry at the carbon atom involved, namely, from retention of configuration for the concerted oxidative insertion (OxIn) to inversion of configuration for the S_N2 pathway. When a stereogenic carbon center is involved in the process, this leads to different enantiomeric products.

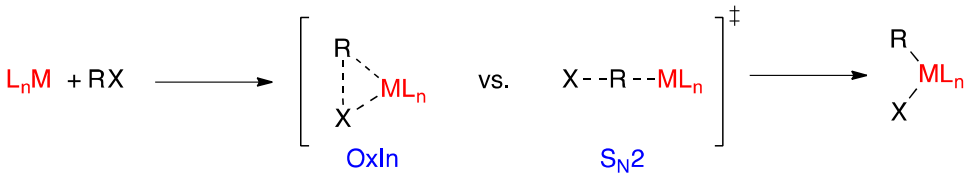

Scheme 2. Proposed reaction mechanisms for the oxidative addition reaction.

The competition between both mechanisms has been studied with the help of the ASM on the gas phase reactions between Pd and CH_3X (X = F to I).[26,27] It was found that the reaction barrier for the oxidative insertion pathway is lower than that for S_N2 substitution. The activation strain diagram in Figure 6 (only the CH_3Cl system is shown) indicates that the more favourable interaction (measured by the ΔE_{int} term) in the OxIn pathway is the major factor controlling the process. This stronger interaction derives from a better overlap between the metal-*d* and substrate σ^*_{C-X} orbitals in the side-on approach, as compared to the back-side approach of the S_N2 pathway.[26,27] Consequently, this causes the S_N2 transition state to occur later, at a point where there is significantly more C–Cl stretch.

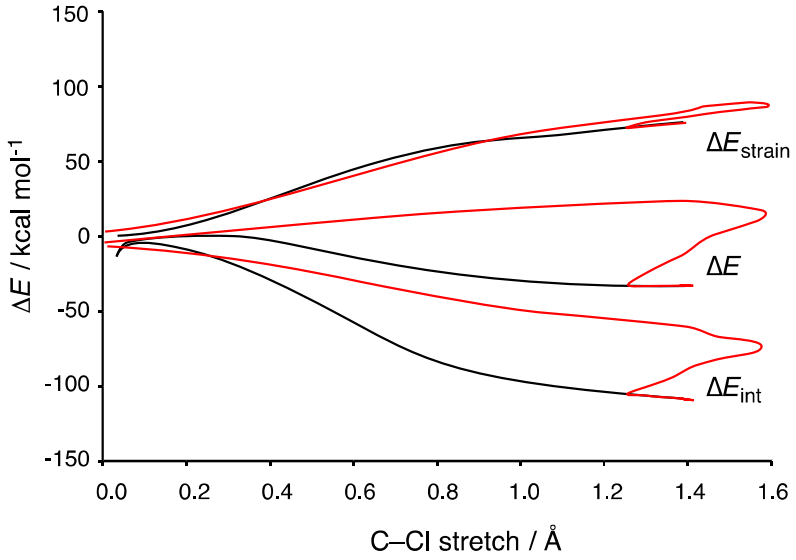

Figure 6. Activation-strain diagram for palladium-induced chloromethane C–Cl bond activation in Pd + CH_3Cl via oxidative insertion (black curves) and via S_N2 substitution (red curves).

Interestingly, anion assistance can shift the reactivity towards the S_N2 pathway.[26] The reason for this inversion in relative reactivity is the aforementioned strengthening of the interaction energy ΔE_{int} that occurs as the Cl^- ligand is coordinated to palladium. Although this effect lowers the barriers of both pathways, the S_N2 pathway "benefits" most because its transition state occurs later along the reaction coordinate, at a point where the ΔE_{int} term is larger and, thus, also its strengthening through anion assistance.

Solvation has opposite effects on the neutral (Pd, no assistance) and anion-assisted ($PdCl^-$) reactions. Indeed, solvation can induce a stronger charge separation across the C–X bond and, thus, a stronger interaction ΔE_{int}. As the S_N2 pathway benefits most from a strengthening in the interaction term (see above), solvation is able to shift oxidative addition to Pd from the OxIn towards the S_N2 pathway. On the other hand, solvation on top of anion assistance shifts reactivity back, from S_N2 to OxIn. The interaction term ΔE_{int} is again responsible. This time, the dominant solvent effect is a stabilization of the charged catalyst complex $PdCl^-$ and a lowering of the energy of its metal *d*-derived frontier orbitals. This diminishes the bonding capabilities of the model catalyst and therefore reduces the stabilizing catalyst–substrate interaction. Again, the S_N2 pathway is most affected by this change in ΔE_{int} which, this time, however, comes down to a weakening. We will come back to the transition metal C–X bond activation through the OxIn mechanism later on, in section 3.3.

3.2. Pericyclic Reactions

Pericyclic reactions constitute an important family of transformations which share a common feature, namely, they proceed concertedly through a fully conjugated cyclic transition state.[28] As they are able to increase the molecular complexity in one single reaction-step, very often with high to complete stereoselectivity, it is not surprising that these reactions are continuously used in organic and organometallic synthesis.

Although Theory has played an important role to understand the intimacies of these concerted transformations (mainly by means of Fukui's popular frontier molecular orbital, or, FMO theory),[4] a significant number of deficiencies have been identified.[29] This is mainly due to the lack of quantitative significance of FMOs as they are often computed only at the equilibrium geometry of the reactants involved. However, by doing so, one ignores how the orbital interactions $\Delta E_{oi}(\zeta)$ evolve along the reaction coordinate ζ as one approaches the transition state region. But it is exactly this behaviour, i.e., the shape of the $\Delta E_{oi}(\zeta)$ curve, that to a great extent determines the height of the activation barrier and its position along the reaction coordinate.

In this section, we present three different types of pericyclic reactions to illustrate the usefulness of the ASM to gain a deeper and quantitative insight into the physical factors which govern these important transformations.

3.2.1. [3+2]-Cycloaddition Reactions involving Heteroallenes

The conversion of heteroallene **1** into the tricyclic compound **3** when reacted with methyl acetylenedicarboxylate (Figure 7), described recently by Escudié and co-workers, attracted our attention.[30] This transformation is suggested to occur via an initial concerted [3+2]-cycloaddition reaction which produces the carbene intermediate **2** followed by a C–H insertion reaction leading to the observed tricyclic compound **3**.

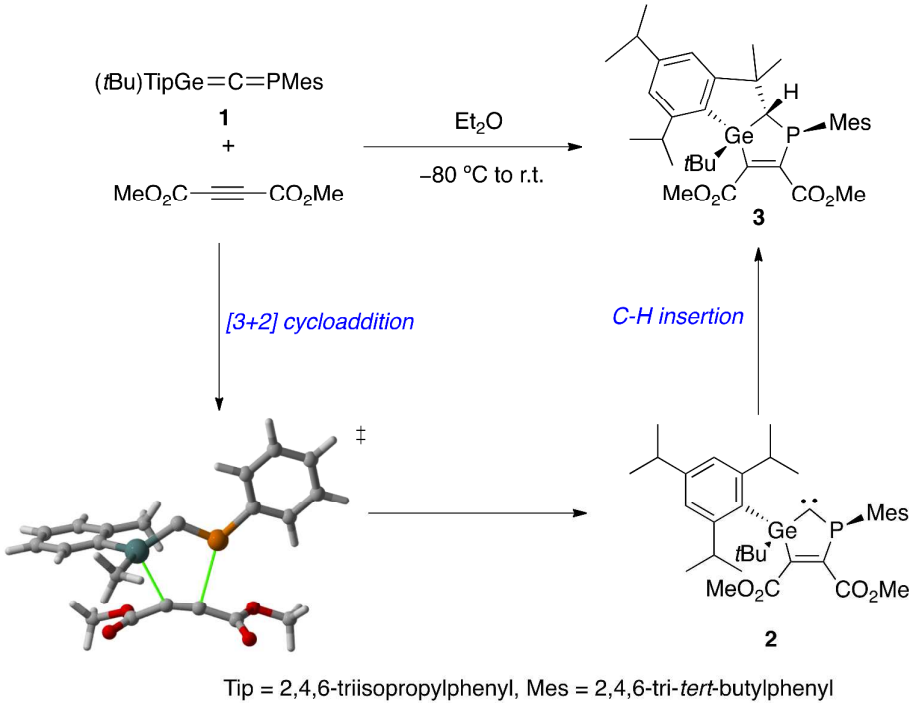

Figure 7. Reaction between heteroallene **1** and methyl acetylenedicarboxylate.

This report prompted us to carry out a comparative study on the effect of group 14 elements in model heteroallenes H_2E=C=PH (E = C to Pb) in their [3+2]-cycloaddition reaction toward acetylene.[31] Our calculations reveal that all the model processes occur concertedly through C_s-symmetric transition states similar to that depicted in Figure 7. Moreover, these saddle points can be considered as in-plane aromatic[32] species in view of the computed negative Nucleus Independent Chemical Shift (NICS) values (in the range of −10 to −21 ppm). Interestingly, the corresponding reaction barriers drop significantly from E = C (nearly 50 kcal/mol) to E = Si-Pb (ca. 20 kcal/mol), which suggests that the process is not feasible when E = C. But what is the origin of this remarkable decrease of the activation barriers when a heavier group 14 element is involved in the cycloaddition?

The ASM gives a quantitative explanation for this differential behaviour. Figure 8 shows the activation strain diagrams for the reactions between acetylene and H_2C=C=PH (solid lines) and H_2Ge=C=PH (dotted lines). In the former case, the reaction profile ΔE raises

monotonically as the reactants approach each other and a sharp increase of ΔE occurs in the proximity of the transition-structure region, leading to the observed high reaction barrier. The interaction energy, ΔE_{int}, which is destabilizing at the beginning of the process, becomes stabilizing at the proximities of the transition state. Despite that, it cannot compensate the strong destabilizing effect of the strain energy and for this reason, a high activation barrier was computed for this process. Differently, in the reaction involving $H_2Ge=C=PH$ as phosphallene, the interaction energy between the deformed reactants remains practically unaltered at long Ge···C distances and then smoothly becomes stabilizing in the vicinity of the transition states. However, the TS interaction energy is not very different in both reactions ($\Delta E^{\ddagger}_{int}$ ca. −10 kcal/mol), which indicates that the strain energy is the major factor controlling the barriers of the [3+2]-cycloadditions. Therefore, the cause that provokes the drop in the reaction barrier is the much lower deformation energy required in the process involving E = Si-Pb. This is mainly due to the fact that heteroallene $H_2C=C=PH$, which possesses a practically linear equilibrium geometry (C=C=P angle of 174.8º), must be bent significantly in the transition state (C=C=P angle of 120.8º). At variance with this, the heteroallenes with a heavier group-14 element E do already possess a bent equilibrium geometry which better fits into the transition state structure and therefore requires less deformation. As a consequence, the latter compounds undergo a significantly more facile (i.e., with a lower barrier) [3+2]-cycloaddition toward acetylene.

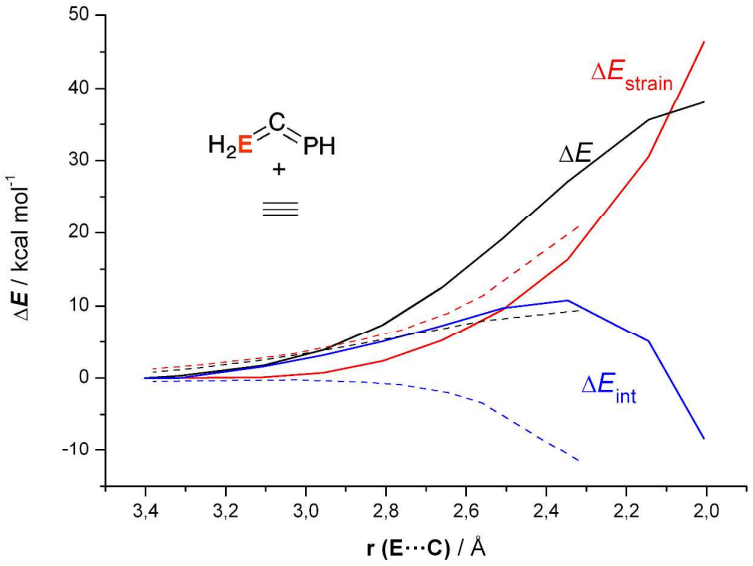

Figure 8. Activation strain analyses for the [3+2]-cycloaddition reaction between acetylene and H_2C=C=PH (solid lines) and H_2Ge=C=PH (dashed lines).

A similar finding, namely, the strain energy as major factor controlling 1,3-dipolar cycloadditions, was found by Houk and Ess when applying the ASM (or distortion/interaction model) to the [3+2]-cycloaddition reactions between different 1,3-dipoles of the type $X=Y^{+}Z^{-}$ (X,Y,Z = first-row elements) and ethylene or acetylene as dipolarophiles (Scheme 3).[8,33] In the majority of cases, the activation strain arises mainly from the deformation of the 1,3-dipole which is associated with the angle change required to achieve the maximum orbital overlap with the corresponding dipolarophile. Moreover, the Houk group has also explored the reaction dynamics of this transformation.[34] Thus, trajectories were propagated in order to ascertain the contributions to the activation barriers from reactant vibration, rotation and relative translation. In good agreement with the above-commented significance of the deformation of the dipole, it was found that the dipole bending modes are extremely important. In fact, the reaction requires a large amount of vibrational excitation in the dipole bending modes in order to occur and these modes contribute greatly to the transition state energy.

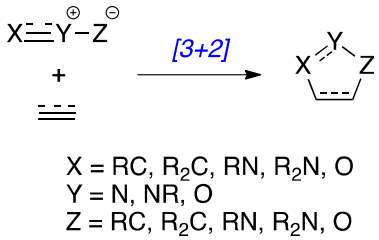

Scheme 3. 1,3-Dipolar cycloaddition reactions studied by Houk and Ess (see references 8 and 33).

3.2.2. Diels-Alder Reaction involving C_{60}

C_{60} fullerene possesses two types of bonds: the pyracylenic type [6,6]-bond, where two six-membered rings are fused, and the corannulenic [5,6]-bond, which corresponds to the ring junction between a five- and a six-membered ring.[35] In general, it is well-known that cycloaddition reactions in empty fullerenes show a remarkable (or exclusive) preference for [6,6]- over [5,6]-bonds. However, the origin of this well-established [6,6]-preference has not been completely understood until a recent ASM study of the [4+2]-cycloaddition between C_{60} and cyclopentadiene.[36] The observed complete [6,6]-regioselectivity of this particular transformation takes place under both kinetic and thermodynamic control, in view of the considerably higher activation energy and less exothermic reaction energy computed for the formation of the corresponding [5,6]-cycloadduct (Figure 9).

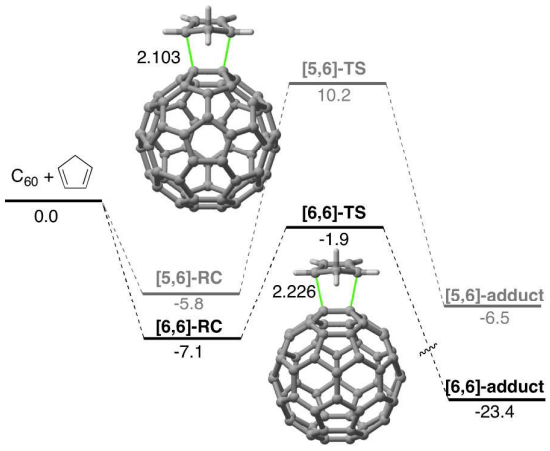

Figure 9. Computed reaction profile of the reaction between cyclopentadiene and C_{60} (taken from reference 36). Energies are given in kcal/mol and bond lengths in angstroms.

Interestingly, the computed TS interactions, $\Delta E^{\ddagger}_{int}$, between the deformed C_{60} and cyclopentadiene are exactly the same (–21.3 kcal/mol) for the [6,6]- and [5,6]-pathways. These single-point analyses in the TS might suggest that the reaction profiles of the two pathways differ due to strain whereas the interaction is the same. However, and as pointed out in Chapter 2, a single-point analysis at the TS only, yields values that can be misleading. Indeed, from the activation strain diagrams in Figure 10, it becomes clear that the stronger interaction between the reactants along the entire reaction coordinate in the [6,6]-reaction pathway is the major factor controlling the selectivity of the process. Thus, the $\Delta E_{int}(\zeta)$ between the deformed reactants is stabilizing from the initial stages of the reaction and becomes more and more stabilizing as one approaches the corresponding transition state. At variance, for the [5,6]-pathway, the reaction profile is initially going up in energy because of a destabilizing interaction $\Delta E_{int}(\zeta)$ between the reactants and inverts at a certain point, after which this term becomes more and more stabilizing as one further approaches the transition state. As a consequence, the [6,6]-transition state is reached earlier than in the [5,6]-pathway and has a lower strain therefore which, in turn, is translated into a much lower activation barrier. The further partitioning of the interaction energy indicates that, similarly to the observed trend in ΔE_{int}, the orbital interactions measured by ΔE_{oi} are always less stabilizing in the [5,6]-pathway along the reaction coordinate. The stronger interactions along the [6,6]-pathway are the result of a more effective <HOMO(cyclopentadiene) | LUMO(C_{60})> overlap, because the (threefold degenerate) LUMO of C_{60} has the appropriate π^* character on [6,6] but not on [5,6] bonds.

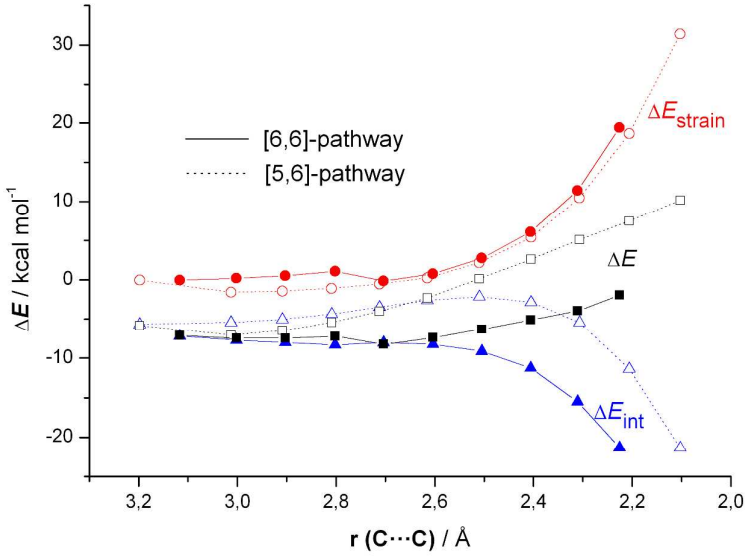

Figure 10. Activation-strain diagram of the [4+2]-cycloaddition reaction between C_{60} and cyclopentadiene along the region comprising the reactant complex and the transition state projected onto the forming C···C bond. Solid lines refer to the [6,6]-pathway whereas dotted lines to the [5,6]-pathway.

In the above example, FMO interactions turn out to be decisive for the observed reactivity. However, there are many situations in which reactivity is *not* orbital-controlled but instead strain-controlled. Traditional FMO theory fails to account for these situations but the ASM model also covers them. A point in case for cycloaddition reactions stems from Houk and co-workers who studied the Diels-Alder reactivity of different cycloalkenes (which exhibit quite similar HOMO–LUMO energies and orbital shapes) with normal and inverse-electron-demand dienes.[37] By means of activation strain (or distortion/interaction) analyses, it was found that the reactivities of cycloalkenes are strain controlled: the strain energy increases with the ring size of the cycloalkenes, resulting in higher activation barriers. Finally, we recently reported that strain, instead of Second Orbital Interactions, is also the major factor behind the well-known endo-rule, empirically formulated by Alder and Stein.[38]

3.2.3. Double Group Transfer Reactions

As a final ASM application to pericyclic reactions, we have selected a family of processes known as Double Group Transfer (DGT) reactions which involve the simultaneous migration of two atoms/groups from one compound to another in a concerted reaction pathway. This definition includes textbook reactions like the diimide reduction of double or triple bonds, the Meerwein-Ponndorf-Verley (MPV) reduction of carbonyl groups, some type II-dyotropic rearrangements which are characterized by the intramolecular migration of the two groups (generally hydrogen atoms),[39] and Alder-ene type reactions.[40] The archetypal DGT reaction is the thermally allowed (according to the Woorward-Hoffmann rules),[3] concerted and highly synchronous [σ2s+σ2s+π2s] suprafacial transfer of two hydrogen atoms from ethane to ethylene. Interestingly, all of these processes share a common feature, namely, they proceed concertedly through highly symmetric six-membered ring transition states which are stabilized by in-plane aromaticity.[41] However, these reactions, in general, are associated with relatively high barriers (typically $\Delta E^{\ddagger} > 40$ kcal/mol),[41,42] which suggests that other factors, which compensate the gain in stability by aromaticity, may control the barrier heights of these transformations. Can we first identify these factors and, afterwards, design lower DGT transformations?

We first considered the parent DGT reaction between ethane and ethylene. The corresponding activation strain diagram projected onto the forming C···H distance show that at the early stages of the process the reaction profile ΔE monotonically becomes more and more destabilized as the reactants approach each other (Figure 11). This initial increase in ΔE is ascribed to the fact that the interaction energy ΔE_{int} between the deformed reactants becomes destabilizing at long H···C distances as a consequence of the Pauli repulsion between closed-shells (notably between the C–H bonds of ethane and the π-system of ethene). In addition, the initial increase in ΔE is also caused by the ethane reactant, as it has to adopt the

required eclipsed conformation to interact with the π-system of ethene. If we now further proceed along the DGT reaction coordinate, the trend in ΔE_{int} inverts at a certain point, after which this term becomes more and more stabilizing. This behaviour resembles that found for other pericyclic reactions but differs for typical S_N2 reactions, where there is a potent HOMO–LUMO interaction from the very beginning of the process leading to a stabilizing interaction energy (see above).

The stabilization in the ΔE_{int} curve occurs shortly after the onset of the strain curve. Despite that, the reason that the overall energy ΔE still goes up until the transition state is of course also the increase in the destabilizing strain energy, which clearly compensates the stabilization provided by ΔE_{int}. This destabilization is ascribed to the breaking of the two C–H bonds in ethane which turns into the dominant contribution to the strain term as the transition state is approached. The partitioning of the ΔE_{int} term indicates that the main contributor to the total interaction between the deformed reactants is the orbital term, ΔE_{oi}, which nicely agrees with the in-plane aromatic character of the corresponding transition state.

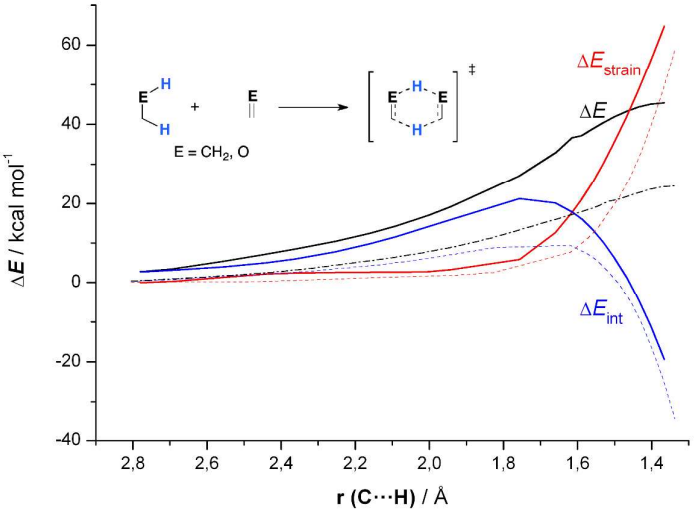

Figure 11. Activation strain analyses of DGT reactions: $H_3C–CH_3$ + $H_2C=CH_2$ (solid curves) and $H_3C–OH$ + $O=CH_2$ (dashed lines).

The above results suggest that it would be possible to design low barrier DGT reactions if we could enhance the interaction energy between the reactants and/or reduce the destabilizing contribution of the strain term. Indeed, for the model MPV reduction of formaldehyde promoted by methanol, the computed activation barrier is significantly reduced to ca. 25 kcal/mol. This is mainly ascribed to the formation of an intramolecular O–H···O=C hydrogen bond that reinforces the interaction between the two reactants (Figure 11). A similar effect has been recently found in ruthenium catalysed Noyori-type hydrogenations of polar double bonds, i.e., ketones, aldehydes and imines.[43] In this particular case, the highly favourable interaction energy between the deformed reactants allows for an easy (barriers ranging from only 9 to 19 kcal/mol) and concerted double hydrogen-atom migration from the Ru–H and N–H bonds via the corresponding six-membered ring transition state (Figure 12).

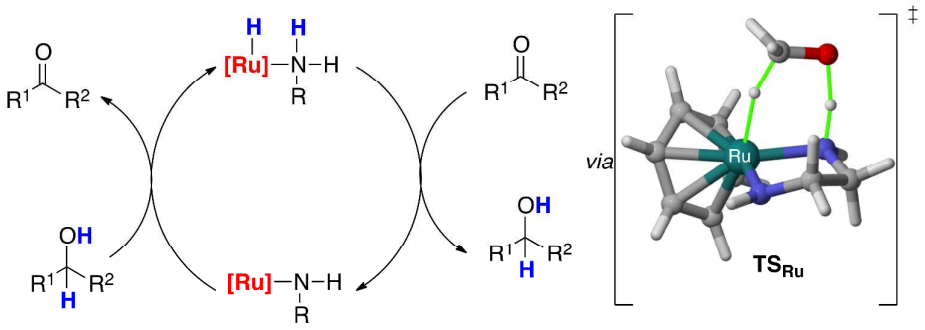

Figure 12. Noyori-type hydrogenation reaction of carbonyl groups.

3.3. Transition Metal Mediated Bond Activation

The activation of C–C, C–H and C–X bonds promoted by transition metal complexes is arguably one of the most valuable methods used in modern synthesis.[44] These processes have not only attracted the attention of synthetic chemists, they have also been deeply studied from a mechanistic point of view, both experimentally and computationally. The purpose of such studies is to obtain an understanding that enables a more rational design of tailor-made catalysts. In this sense, the activation strain model has been thoroughly applied to these

transformations to gain insight into how variations in the substrates, transition metal and the ligands in its coordination sphere affect the activation barriers of the different oxidative addition reactions.

3.3.1. Substrate Effects on Bond Activation

An illustrative example of the substrate effect is the comparison of the oxidative insertion reaction of palladium into the C–C bond of ethane and cyclopropane (Figure 13). The weaker C–C bond in the highly strained cyclopropane ring results in a much easier insertion process. Thus, whereas a value of ca. 18 kcal/mol was computed for the insertion into the C–C bond of ethane, the process occurs practically without any measurable barrier for cyclopropane.[27]

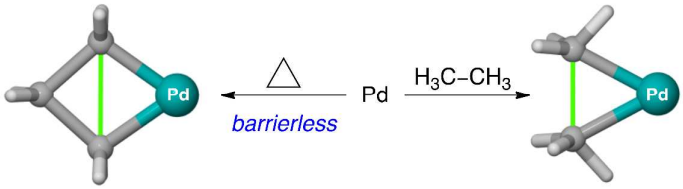

Figure 13. Oxidative insertion of palladium into the C–C bond in ethane and cyclopropane.

The ASM shows that the weakening of the C–C bond caused by ring strain in turn lowers the insertion barrier because of a lower activation strain $\Delta E^{\ddagger}_{strain}$. This finding is in line with results of Houk and co-workers on the Diels-Alder reactions involving cycloalkenes.[37] In addition, it appears that the strained system also allows for an easier access of the palladium to the C–C bond. In the ethane oxidative insertion, the hydrogen atoms on the methyl groups have to bend away in order to allow contact of palladium with the C–C bond. The interaction with the bond is thus greatly reduced due to steric shielding of the methyl groups. In cyclopropane this bending away of the hydrogen atoms is already built into the geometry of the substrate, thus allowing for stronger interaction early along the entire reaction

coordinated. As a result, both the strain and interaction terms are stabilized for the oxidative insertion into cyclopropane as compared to the situation for ethane (see Figure 14).

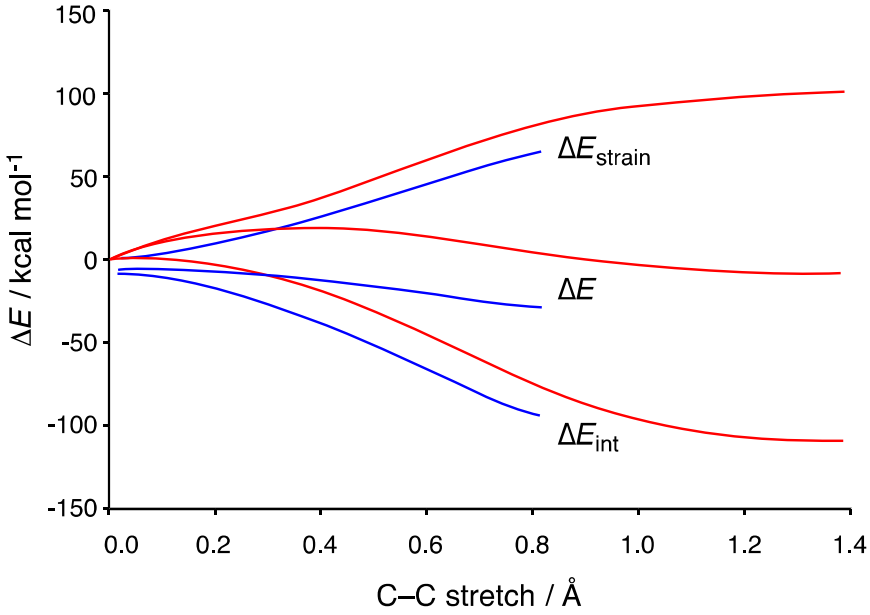

Figure 14. Activation strain diagram for oxidative insertion of Pd into the ethane C–C (red curves) and cyclopropane C–C bond (blue curves).[27]

It is interesting to compare the C–C bond activation with the corresponding oxidative insertion into the methane C–H bond, shown in Figure 15. Our calculations indicate that the methane C–H activation barrier is ca. 14 kcal/mol lower despite the fact that this bond is much stronger than the C–C bond. The reason for the low C–H activation barrier is similar to that found for the C–C bond in cyclopropane: there is very little steric shielding on the side of the hydrogen, so interaction with the C–H bond proceeds easily, right from the beginning. At variance, the C–C bond is shielded on both ends by the methyl C–H bonds which prevent the palladium atom to approach and "electronically touch" the C–C bond for some time.[26,27] Only after the C–C bond has been sufficiently elongated and the methyl groups have tilted away, there is room for the metal atom to come closer and build up overlap between its *d* orbitals and the C–C σ^* acceptor orbital. The initial delay in metal–substrate interaction ΔE_{int} in the case of the ethane C–C activation can be clearly seen in Figure 15. On the other hand, the

computed low reaction barrier for the palladium-mediated activation of C–Cl bond as compared to C–H bond can be explained straightforwardly by the much lower C–Cl bond strength, which manifests itself in a less destabilizing ΔE_{strain} curve.[27]

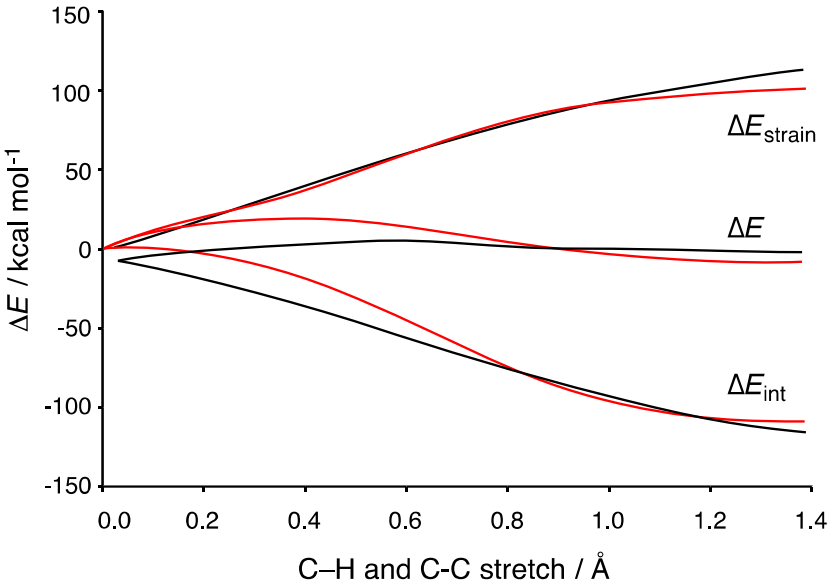

Figure 15. Activation strain diagram for oxidative insertion of Pd into the ethane C–C (red curves) and methane C–H bond (black curves).[27]

3.3.2. Ligand Effects on Bond Activation

The ASM has been particularly helpful to understand the strong influence of the ligands directly attached to the palladium center. Thus, the C–H, C–C and C–Cl bond activations promoted by differently coordinated palladium(0) complexes, covering a broad spectrum of monodentate and chelate complexes of palladium with simple, bulky and halogen-substituted diphosphine as well as *N*-heterocyclic carbene ligands, have been thoroughly studied.[45]

It is well-known that the catalyst's activity strongly depends on the ligand–metal–ligand bite angle. The common explanation is that, as a result of the bending of the complex away from linearity, the ligand lone pairs push the metal *d* orbital up in energy, thus, strengthening the HOMO–LUMO interactions with the substrate's σ^* acceptor orbital. As a

consequence of the more stabilizing interaction between catalyst and substrate, the activation energy for metal complexes with smaller bite angles should be lower.

However, the ASM reveals that this electronic bite-angle mechanism is not really the origin of the observed reactivity. Differently, the bite angle effect rather has a geometrical or steric nature as illustrated in Figure 16, which compares the methane C–H bond activation by Pd and $Pd(PH_3)_2$. Our calculations indicate that the introduction of phosphine ligands raises the barrier, that is, it makes the catalyst less active. This appears to come from both, increased strain ΔE_{strain} and less stabilizing interaction ΔE_{int}, as suggested by the corresponding activation strain diagrams (Figure 16). Closer inspection reveals that both effects have a common origin: the phosphine ligands experience steric (Pauli) repulsion with the substrate, and this repulsion increases as the oxidative-addition reaction proceeds. This, in turn, causes the interaction to become less favourable. At the same time, part of the steric repulsion is relieved by the phosphine ligands bending away from the substrate. This shows up in an additional amount of strain, building up at the beginning of the reaction path, which stems from the catalyst's bending deformation.

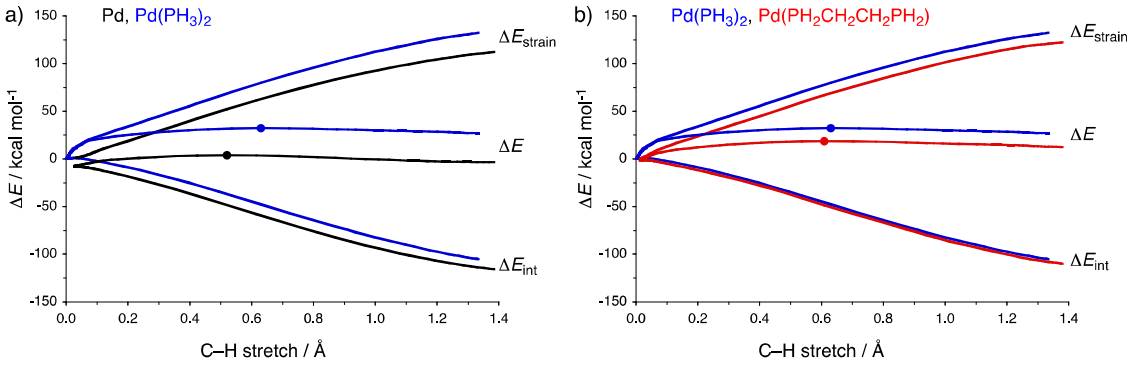

Figure 16. Activation strain diagrams for methane C–H activation by: a) Pd (black) *vs.* $Pd(PH_3)_2$ (blue); and b) by $Pd(PH_3)_2$ (blue) *vs.* $Pd(PH_2CH_2CH_2PH_2)$.

Results above indicate that by bending the catalyst a priori, the unfavourable non-bonded interactions with the substrate, which cause the catalyst to deform and build up strain,

can be avoided, thus leading to a more efficient process. This is what happens when we introduce a short bridge connecting the two phosphine centers in a bidentate ligand, and in general, in chelate complexes. Interestingly, the increased strain in short-bridged palladium chelate complexes has also been demonstrated in the context of catalyst selection through mass spectrometry, based on the catalyst's intrinsic stability.[46] Apart from that, this initial bending of the catalyst can be induced by modifying the transition metal as well. As recently reported, the expected linear ligand–metal–ligand (L-M-L) angle in d^{10}-ML_2 complexes (M = Co^-, Rh^-, Ir^-, Ni, Pd, Pt, Cu^+, Ag^+, Au^+; L = NH_3, PH_3, CO) varies from the more common 180º to values as small as 129º as a function of the metal as well as the ligands.[47] This "bending effect", which is driven by π-backdonation and opposed by steric repulsion, may have potential implications in the activation barriers of bond activation reactions.

Houk and co-workers have quite recently highlighted the usefulness of the ASM to understand bond activations promoted by transition metal complexes. Thus, the origins of the chemoselectivity of Ni-catalysed C−O activation of aryl esters have been explored (Scheme 4).[48] It was found that, for aryl esters, nickel with bidentate phosphine ligands cleaves C(acyl)−O and C(aryl)−O bonds via three-centered transition states. The C(acyl)−O activation is favoured due to the lower bond dissociation energy of the C(acyl)−O bond, which translates into a lower activation strain $\Delta E^{\ddagger}_{strain}$ (or transition-state distortion energy). However, when monodentate phosphine ligands are used, a vacant coordination site on nickel creates an extra Ni−O bond in the five-centered C(aryl)−O cleavage transition state. As a result of this additional interaction, the ΔE_{int} between the deformed catalyst and substrate favours the C(aryl)−O activation.

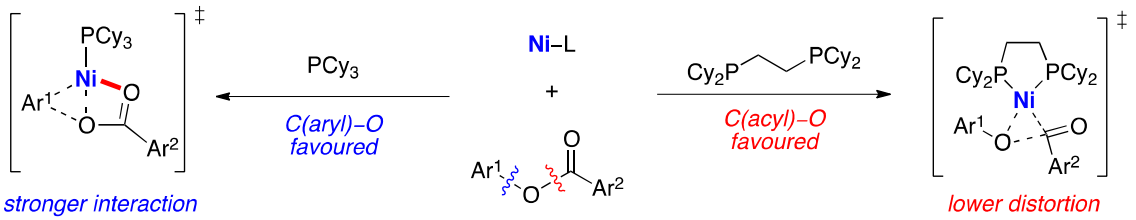

Scheme 4. Chemoselectivity of Ni-catalysed C−O activation of aryl esters.

4. Extension to Unimolecular Processes

An initial limitation of the ASM was that it had been originally conceived to study bimolecular reactions which correspond to a two-fragment picture (like all the transformations described in the previous section). But this does not necessarily mean that intramolecular reactions cannot be analysed by the ASM. On the contrary, by using a careful and chemically meaningful fragmentation scheme, unimolecular reactions can be studied as well. To illustrate this, we present the following final examples recently considered by us: (i) type-I dyotropic reactions[49] and (ii) cyclization reactions of ene-ene-ynes.[50]

4.1. Type-I dyotropic reactions

Type-I dyotropic reactions are a particular class of DGT reactions which involve the intramolecular and simultaneous migration of two σ-bonds. In these rearrangements, the migrating atoms or groups interchange their relative molecular positions, at variance with type-II processes, where the migration does not involve positional interchange.[39] A well known representative of type-I dyotropic reaction is the 1,2-shift occurring in vicinal dibromides, which proceeds through a four-membered ring transition state with inversion of configuration at both carbon atoms (Figure 17). This interesting reaction can be conceived as the interconversion between two very strongly bound reactant complexes of X_2 + $H_2C{=}CH_2$.[49] In fact, the progress of the reaction indeed strongly resembles a rotation of the [X···X] fragment relative to the $H_2C{=}CH_2$ fragment. This approach turns out to provide detailed

insight into trends in activation energies by separating them into trends in X_2 and $H_2C{=}CH_2$ rigidity and C–X bonding. In this picture, the barrier of the 1,2-dyotropic reaction arises from the *change* in strain of and in interaction between X_2 and $H_2C{=}CH_2$ as one goes from $\tilde{X}CH_2\tilde{C}H_2\tilde{X}$ to the corresponding four-membered ring transition state. Therefore, in this particular case: $\Delta E^{\ddagger} = \Delta\Delta E_{strain}^{\ddagger} + \Delta\Delta E_{int}^{\ddagger}$.

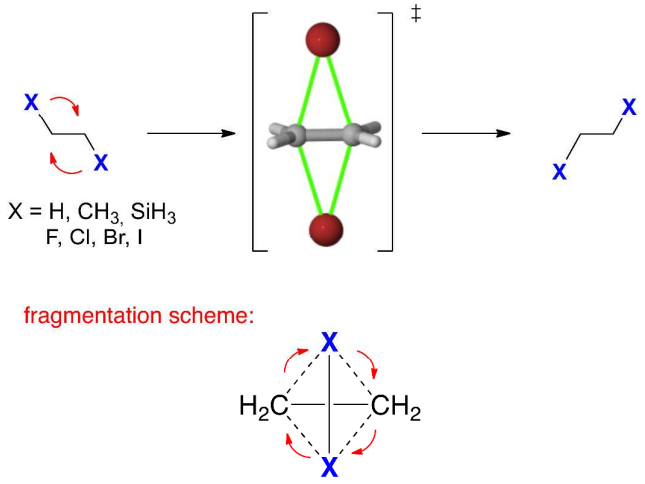

Figure 17. Type-I dyotropic reaction in 1,2-disubstituted ethanes.

Our comparative study of the relative migratory aptitude of the X atom/group indicate that the weakening in the interaction energy $\Delta\Delta E_{int}$, that derives from partial C–X bond breaking in the transition state, constitutes the major factor controlling the barrier of the 1,2-dyotropic migration. This result indicates that the trends in reactivity on variation of X in these particular 1,2-shifts (migratory aptitude of X: H < CH_3 < SiH_3 << F < Cl< Br < I) can be understood, *i.a.*, in terms of how sensitive the C–X interaction is towards adopting the transition state geometry. In other words: the softer the C–X bond, the lower the barrier.

4.2. Ene-Ene-Yne Cyclization Reactions

We were interested in understanding the thermal cycloisomerization reactions of 1,3-hexadien-5-ynes into isobenzene (also known as Hopf cyclization), a process analogous to the

well-known Bergman cyclization of *cis*-3-hexene-1,5-diynes (Figure 18).[50] For the parent reaction involving cis-1,3-hexadiene-5-yne, we used the CH_2=CH· and ·CH=C-CH≡CH as fragments, calculated in the electronic doublet state with the unpaired electron in a σ-sp^2 orbital. This approach provides insight into trends in activation energies in terms of rigidity and mutual bonding (in particular new C···C bond) of both fragments. In this picture, the reactant ene-ene-yne is a "very strongly bound reactant complex" where the barrier of the cyclization reaction arises again from the *change* in strain ($\Delta\Delta E^{\ddagger}_{strain}$), and in the *change* in interaction ($\Delta\Delta E^{\ddagger}_{int}$) between these radical fragments as one goes from the initial reactant to the corresponding transition state.

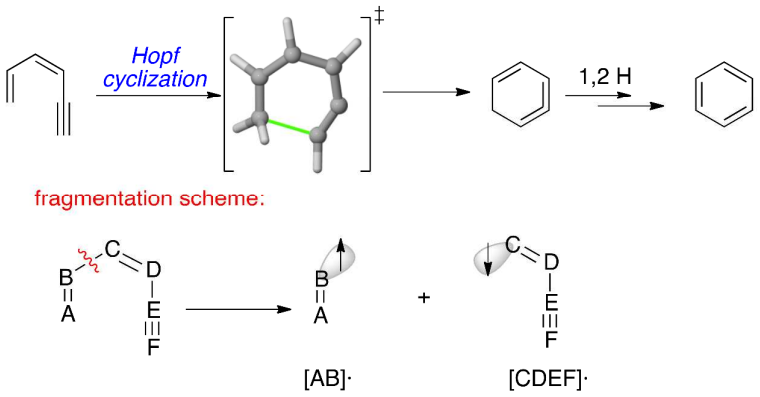

Figure 18. Cycloisomerization reactions of 1,3-hexadien-5-ynes.

The ASM applied to different starting ene-ene-ynes of the type A=B-C=D-E≡F shows that the major factor controlling the corresponding Hopf cyclization is the geometrical strain energy associated with the rotation of the terminal [A] group. This rotation is necessary for achieving a favourable HOMO-LUMO overlap with the yne-moiety [F] associated with the formation of the new A–F single bond. Thus, when this terminal [A] group features a heteroatom (O or NH), such a rotation is no longer required and, as a consequence, the total activation strain collapses and the corresponding energy barriers become much lower than when group [A] corresponds to a CH_2 or CHMe group.

5. Concluding Remarks and Outlook

A model of chemical reactivity must be rooted in quantum mechanics, provide insight, and posses predictive power.[51] The mere measurement or computation of a rate or barrier does not suffice if one wishes to understand and design new chemical processes. As we have shown along this Tutorial Review, the activation strain model (ASM) of chemical reactivity satisfies these conditions. It constitutes a quantitatively accurate causal relationship between reaction barriers, on one hand, and the nature of reactants, the type of chemical transformation, as well as the medium in which it proceeds. The ASM does so by conceiving the potential energy surface $\Delta E(\zeta)$ along the reaction coordinate ζ as being constituted by the strain $\Delta E_{\text{strain}}(\zeta)$ of the increasingly deformed reactants plus the interaction $\Delta E_{\text{int}}(\zeta)$ between these deformed reactants, i.e., $\Delta E(\zeta) = \Delta E_{\text{strain}}(\zeta) + \Delta E_{\text{int}}(\zeta)$. This decomposition can be done using any quantum chemical program.

In various applications to organic and organometallic (catalysis) chemistry, we have brought the model to life. Universal concepts arise, such as the mutual capability of reactants which can be tuned by their composition (cf. anion-assistance in catalysis, pH in competing organic reactions) or by the choice of solvent (solvation, for example, reduces the electron-donating capability of a reactant). Another concept is the activation strain, the strain energy associated with the deformation that reactants undergo during the process. It depends on the sterics and the flexibility or rigidity of the reactants involved as well as on the distortivity, i.e., the characteristic extent of deformation, associated with a particular chemical transformation.

The ASM is thus a unifying approach to uni- and bimolecular reactions which incorporates, but also extends far beyond, FMO theory. Together with the associated concepts, it constitutes a toolbox not only for understanding but also for designing chemical reactions.

Acknowledgments. This work was supported by the Netherlands Organization for Scientific Research (NWO/CW), the National Research School Combination - Catalysis (NRSC-C), and by the Spanish MINECO and CAM (Grants CTQ2010-20714-C02-01, Consolider-Ingenio 2010, CSD2007-00006 and S2009/PPQ-1634).

References and Notes

[1] L. Pauling, *General Chemistry*. Dover Publications, Inc., 1947.
[2] K. C. Nicolaou and T. Montagnon, *"Molecules that Changed the World"*, Wiley-VCH, 2008.
[3] R. B. Woodward and R. Hoffmann, *The Conservation of Orbital Symmetry*, Verlag, Chemie, GmbH: Weinheim, 1970.
[4] K. Fukui, *Acc. Chem. Res*., 1971, **4**, 57, and references therein.
[5] S. Shaik and P. C. Hiberty, *A Chemist's Guide to Valence Bond Theory,* Wiley-Interscience, Hoboken, New Jersey, 2007.
[6] R. A. Marcus, *Annu. Rev. Phys. Chem*., 1964, **15**, 155.
[7] F. M. Bickelhaupt, *J. Comput. Chem*., 1999, **20**, 114.
[8] D. H. Ess, K. N. Houk, *J. Am. Chem. Soc.,* 2007, **129**, 10646.
[9] W-J. Van Zeist and F. M. Bickelhaupt, *Org. Biomol. Chem*., 2010, **8**, 3118.
[10] (a) F. M. Bickelhaupt and E. J. Baerends, In: *Reviews in Computational Chemistry* (K. B. Lipkowitz and D. B. Boyd, Eds.); Wiley-VCH: New York, 2000, Vol. 15, pp. 1-86. See also: (b) T. Ziegler and A. Rauk, *Theor. Chim. Acta*, 1977, **46**, 1. (c) K. Morokuma, *J. Chem. Phys.*, 1971, **55**, 1236.
[11] C. González and H. B. Schlegel, *J. Phys. Chem*., 1990, **94**, 5523, and references therein.
[12] (a) *Amsterdam Density Functional* program, Scientific Computing & Modelling NV. Vrije Universiteit, Amsterdam: *www.scm.com*. (b) G. te Velde, F. M. Bickelhaupt, E. J. Baerends, C. Fonseca Guerra, S. J. A. van Gisbergen, J. G. Snijders, T. Ziegler, *J. Comput. Chem.* **2001**, *22*, 931.
[13] C. K. Ingold, *Structure and Mechanism in Organic Chemistry*, Cornell University, Ithaca, 1953.
[14] A. P. Bento and F. M. Bickelhaupt, *J. Org. Chem.*, 2007, **72**, 2201.
[15] The picture emerging from the ASM is also confirmed by the ball-in-a-box (BiaB) model: S. C. A. H. Pierrefixe, C. Fonseca Guerra and F. M. Bickelhaupt, *Chem. Eur. J.*, 2008, **14**, 819.
[16] A. P. Bento and F. M. Bickelhaupt, *J. Org. Chem.*, 2008, **73**, 7290.
[17] M. A. van Bochove, M. Swart and F. M. Bickelhaupt, *J. Am. Chem. Soc.*, 2006, **128**, 10738.
[18] S. C. A. H. Pierrefixe, S. J. M. van Stralen, J. N. P. van Stralen, C. Fonseca Guerra and F. M. Bickelhaupt, *Angew. Chem. Int. Ed*., 2009, **48**, 6469.
[19] I. Fernández, G. Frenking and E. Uggerud, *J. Org. Chem.*, 2010, **75**, 2971.
[20] I. Fernández, F. M. Bickelhaupt and E. Uggerud, *J. Org. Chem*., 2013, **78**, 8574.
[21] (a) I. Fernández, G. Frenking and E. Uggerud, *Chem. Eur. J.,* 2009, **15**, 2166. (b) W.-J. van Zeist, F. M. Bickelhaupt, *Chem. Eur. J.* **2010**, *16*, 5538.
[22] L. P. Wolters, Y. Ren and F. M. Bickelhaupt, *ChemistryOpen*, 2014, **3**, 29.

[23] X.-P. Wu, X.-M. Sun, X.-G. Wei, Y. Ren, N.-B. Wong and W.-K. Li, *J. Chem. Theory Comput.*, 2009, **5**, 1597.
[24] S. Y. Yun, S. Catak, W. K. Lee, M. D'hooghe, N. De Kimpe, V. Van Speybroeck, M. Waroquier, Y. Kim and H.-J. Ha, *Chem. Commun.*, 2009, 2508.
[25] For a recent review, see: M. García-Melchor, A. A. C. Braga, A. Lledós, G. Ujaque and F. Maseras, *Acc. Chem. Res*., 2013, **46**, 2626 and references therein.
[26] G. T. de Jong and F. M. Bickelhaupt, *J. Chem. Theory Comput.*, 2007, **3**, 514.
[27] G. T. de Jong and F. M. Bickelhaupt, *ChemPhysChem*, 2007, **8**, 1170.
[28] S. Sankararaman, *Pericyclic Reactions–A Textbook: Reactions, Applications and Theory*; Wiley: Weinheim, 2005.
[29] For a review, see: D. H. Ess, G. O. Jones and K. N. Houk, *Adv. Synth. Catal*., 2006, **348**, 2337.
[30] D. Ghereg, E. André, J.-M. Sotiropoulos, K. Miqueu, H. Gornitzka and J. Escudié, *Angew. Chem. Int. Ed*., 2010, **49**, 8704.
[31] I. Fernández, F. M. Bickelhaupt and F. P. Cossío, *J. Org. Chem.,* 2011, **76**, 2310.
[32] For a description of in-plane aromaticity, see: F. P. Cossío, I. Morao, H. Jiao and P. v. R. Schleyer, *J. Am. Chem. Soc.,* 1999, **121**, 6737.
[33] D. H. Ess and K. N. Houk, *J. Am. Chem. Soc.,* 2008, **130**, 10187.
[34] L. Xu, C. E. Doubleday and K. N. Houk, *Angew. Chem., Int. Ed*., 2009, **48**, 2746.
[35] *Fullerenes. Principles and Applications* (Eds.: F. Langa, J.-F. Nierengarten), RSC, Cambridge, 2011 and references therein.
[36] I. Fernández, M. Solà and F. M. Bickelhaupt, *Chem. Eur. J.*, 2013, **19**, 7416.
[37] F. Liu, R. S. Paton, S. Kim, Y. Liang and K. N. Houk, *J. Am. Chem. Soc*., 2013, **135**, 15642.
[38] I. Fernández and F. M. Bickelhaupt, *J. Comput. Chem*., 2014, **35**, 371.
[39] For a recent review on dyotropic reactions, see: I. Fernández, F. P. Cossío and M. A. Sierra, *Chem. Rev*., 2009, **109**, 6687.
[40] I. Fernández and F. M. Bickelhaupt, *J. Comput. Chem.*, 2012, **33**, 509.
[41] I. Fernández, M. A. Sierra and F. P. Cossío, *J. Org. Chem.*, 2007, **72**, 1488.
[42] I. Fernández, F. M. Bickelhaupt and F. P. Cossío, *Chem. Eur. J.*, 2009, **15**, 13022.
[43] O. Nieto Faza, C. Silva López and I. Fernández, *J. Org. Chem*., 2013, **78**, 5669.
[44] For instance, see the recent issue on C–H bond activation, *Acc. Chem. Res*., 2012, **45**.
[45] W-J. Van Zeist and F. M. Bickelhaupt, *Dalton Trans.*, 2011, **40**, 3028 and references therein.
[46] J. Wassenaar, E. Jansen, W.-J. van Zeist, F. M. Bickelhaupt, M. A. Siegler, A. L. Spek and J. N. H. Reek, *Nature Chem*., 2010, **2**, 417.
[47] L. P. Wolters and F. M. Bickelhaupt, *ChemistryOpen*, 2013, **2**, 106.
[48] X. Hong, Y. Liang and K. N. Houk, *J. Am. Chem. Soc*., 2014, **136**, 2017.
[49] I. Fernández, F. M. Bickelhaupt and F. P. Cossío, *Chem. Eur. J.,* 2012, **18**, 12395.
[50] I. Fernández, F. M. Bickelhaupt and F. P. Cossío, *Chem. Eur. J.,* 2014, doi: 10.1002/chem.201303874.
[51] J. Poater, M. Solà and F. M. Bickelhaupt, *Chem. Eur. J.*, 2006, **12**, 2902.

Biographical Sketches

Matthias Bickelhaupt holds chairs in theoretical organic chemistry at VU University Amsterdam and Radboud University Nijmegen. He is head of the Department of Theoretical Chemistry at VU University, Chairman of the Board of the Amsterdam Center for Multiscale Modeling (ACMM) and Chairman of the Hoalland Research School of Molecular Chemistry (HRSMC). M.B. received his MSc with Evert Jan Baerends (VU University Amsterdam), his PhD with Nico Nibbering (University of Amsterdam) and Evert Jan Baerends, and was a postdoctoral associate in the groups of Paul von Ragué Schleyer (Erlangen, Germany), Tom Ziegler (Calgary, Canada) and Roald Hoffmann (Cornell University, USA). In 1997, he was appointed assistant professor in Marburg, Germany, and obtained tenure in 1999 at VU University in Amsterdam. M.B.'s research interests cover a broad range of topics in the fields of molecular structure and chemical bonding, biochemistry, reactivity, and catalysis.

Israel Fernández (Madrid, 1977) studied Chemistry at the Universidad Complutense of Madrid (UCM). In 2005, he earned his Ph.D. (with honors) at the UCM under the supervision of Prof. Miguel A. Sierra receiving the Lilly-Young Researcher Award. After that, he joined the Theoretical and Computational Chemistry group of Prof. Gernot Frenking at the Philipps Universität Marburg as a postdoctoral researcher. In 2009, he received the Young-Researcher Award from the Spanish Royal Society of Chemistry and the Julián Sanz del Río award in 2011. At present, I.F. is *Profesor Contratado Doctor* at the UCM. His current research includes the experimental and computational study of the bonding situations and reaction mechanisms of organic and organometallic compounds with special interest in C̄C bond forming processes.

.